
Proceedings of the Symposium K: "Complex Oxide Materials for New Technologies"
of E-MRS Fall Meeting 2006, Warsaw, September 4–8, 2006

Surfactant Effect on Synthesis of Nanocrystalline $\text{La}_x\text{Sr}_{1-x}\text{MnO}_3$ by Hydrothermal Method

W.L. SIN^a, K.H. WONG^a AND P. LI^b

^aDepartment of Applied Physics, The Hong Kong Polytechnic University
Kowloon, Hong Kong

^bDepartment of Applied Biology and Chemical Technology
The Hong Kong Polytechnic University, Kowloon, Hong Kong

Crystalline $\text{La}_x\text{Sr}_{1-x}\text{MnO}_3$ was prepared by a hydrothermal route in the presence of surfactant. The cationic surfactant of cetyltrimethylammonium bromide as a template is used to regulate the nucleation and crystal growth. The as-synthesized product was characterized by X-ray diffraction and transmission electron microscopy. Nanosized and uniform rod-like monocrystals of $\text{La}_x\text{Sr}_{1-x}\text{MnO}_3$ were obtained. Their magnetic properties were studied using a vibrating sample magnetometer. Our results reveal that the use of surfactant helps to lower the processing temperature and to speed up the formation and crystallization of $\text{La}_x\text{Sr}_{1-x}\text{MnO}_3$. The surfactant also provides us an additional means of controlling the nanocrystalline size and maintaining the stoichiometry of the as-prepared nanocrystallites.

PACS numbers: 75.47.Lx, 82.70.Uv, 61.10.Nz

1. Introduction

In recent years there has been a great interest in the study of perovskite manganites $\text{A}_x\text{B}_{1-x}\text{MnO}_3$, and its related material systems [1]. The attraction originated from the unexpectedly large magnetotransport properties of these compounds. Upon the application of small magnetic field, the resistivity changes by many orders of magnitude, an effect that carries the name of colossal magnetoresistance (CMR) [2]. Manganites also exhibit a variety of phases, with unusual spin, charge, lattice, and orbital order [1]. A large number of experiments on polycrystals [3], single crystals [4] and thin films [5] have been carried out to study the physics involved and to explore possible applications of CMR effect.

Among the manganites, $\text{La}_{0.3}\text{Sr}_{0.7}\text{MnO}_3$ (LSMO) is one of the manganese oxide compounds that has received the most attention [6]. Using a magnetotransport measurement, at least 95% spin polarization has been reported in thin film of $\text{La}_{0.3}\text{Sr}_{0.7}\text{MnO}_3$ [7]. This material has a large Curie temperature as high as 370 K [6]. Over the past decades, it has been extensively studied in bulk or in thin film forms. In-depth understanding has been developed on issues such as the correlation of the transition temperature to the material composition.

On the other hand, nanomagnetic materials have generated continuous interest since 1940s as the study of their properties turned out to be challenging from both scientific and technological point of view [7]. Nanosize LSMO will definitely be an interesting material due to its special properties. For example, manganite polycrystallites with small grain sizes exhibit pronounced CMR under a low applied field over a wide temperature range [8].

Recently several colloidal chemical synthetic procedures have been developed to produce monodisperse nanoparticle. Manganite such as LSMO can be synthesized by many chemical-processing routes including solid state reaction [9], coprecipitation [10], sol-gel synthesis [11], microemulsion [12] and hydrothermal reaction [13]. Among them, the hydrothermal synthesis method is able to synthesize a fine, crystalline, and de-agglomerated powder at lower temperatures. However, due to the vastly diversified crystallization temperature and chemical reaction conditions, the stoichiometry of the as-synthesized nano-crystallite of complex oxides is difficult to control.

It is known that the size of nanoparticles can be controlled easily through the use of tailed surfactants in the system. Here we reported an effort to employ the surfactant template for controllable synthesis of LSMO nanoparticles. Metal chloride solution was reacted and precipitated in the presence of KMnO_4 and the cationic surfactant of cetyltrimethylammonium bromide (CTAB). CTAB in the chemical formula of $((\text{C}_{16}\text{H}_{33})\text{N}(\text{CH}_3)_3\text{Br})$ is one of the most important surfactants. It consists of a straight 16-carbon aliphatic chain with the quaternary ammonium group as the terminal group at one end. The presence of CTAB in solution caused the formation of positive charge droplets that enhanced electrostatic interactions between emulsion and the reactant species [14]. Surfactants reduce the surface tension of water being absorbed at the air-water interface. They also reduce the interfacial tension between oil and water being absorbed at the liquid-liquid interface. Many surfactants can also assemble in the bulk solution into aggregates that are known as micelles.

2. Experimental details

2.1. Material and methods

Analytical grade KMnO_4 , $\text{MnCl}_2 \cdot 4\text{H}_2\text{O}$, $\text{LaCl}_3 \cdot 7\text{H}_2\text{O}$, $\text{SrCl}_2 \cdot 6\text{H}_2\text{O}$ were used as starting materials. The reactions were performed in 10 ml teflon-lined stainless steel autoclaves. KOH was added to maintain a proper alkalinity. Then,

the CTAB powder was mixed with the above solution containing metal ions and agitated vigorously to obtain a homogeneous black solution. The reaction mixture was placed in the autoclaves and heated at 240°C under the autogenously pressure for 1 day. The results was a colloidal solution of black colored nanocrystalites, which were then filtered off and washed with ethanol and deionized water mixed in the volume ratio 1:8 to remove the residual CTAB, potassium ions, and chloride ions. The final product was then dried at 80°C for 2 hours to yield a small quantity of black powder.

2.2. Characterization

The synthesized nano-powders were characterized using X-ray powder diffractometer (XRD) (Philips X'pert XRD system) and transmission electron microscopy (TEM). The specific magnetization of the powders was measured using a vibrating sample magnetometer. The nanoparticles were deposited on a copper grid supported with transparent carbon foil. The samples were examined by a conventional TEM (JEOL 2010 microscope) operating at 200 kV. Apart from direct observations using the TEM, the particle size of the product was estimated from the broadening of the XRD peak using “Debye–Scherrer method”.

3. Results and discussions

Figure 1 shows the XRD pattern of LSMO samples obtained at different contents of CTAB cationic surfactant. In general, all the XRD patterns correspond to the characteristic peaks of LSMO. For sample prepared with 0.2 g CTAB

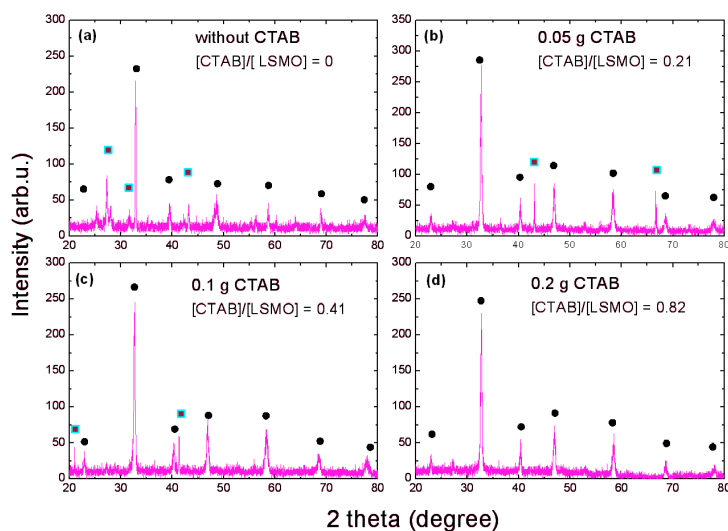


Fig. 1. X-ray powder diffraction pattern of LSMO nanoparticles produced in the presence of CTAB with different quantities: (a) no CTAB, (b) 0.05 g CTAB, (c) 0.10 g CTAB and (d) 0.20 g CTAB (● LSMO phase, □ impurities phase).

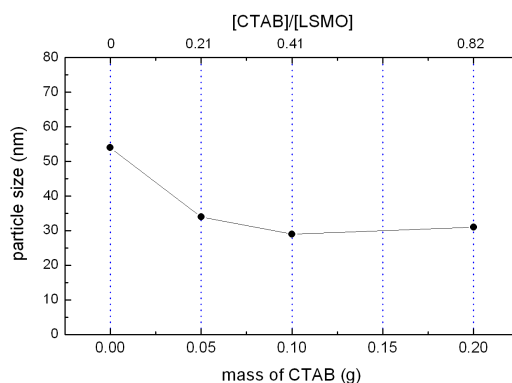


Fig. 2. Variation of the particle size as a function of content of CTAB surfactant.

([CTAB]/[LSMO] = 0.822), a single phase crystalline powder was obtained directly by the hydrothermal process. The cubic lattice parameter calculated from the scan of (110) reflection is found to be 0.386 nm, which matches with the reported bulk value. For the lower content of CTAB, a trace amount of impurities phases were produced although the formation of perovskite LSMO with high crystallinity is evident. The existence of impurities in the product indicates that the reaction has not been completed. The (002) lines of the diffraction pattern were used to calculate the particle size via Scherrer equation ($D = 0.94\lambda / (\text{FWHM}\cos\theta)$) where D — the particle size, λ — the X-ray wavelength, FWHM — the line broadening and θ — the Bragg angle. Figure 2 shows the plot of particle size versus the content of cationic surfactant CTAB. The particle size decreases gradually from 54 nm (0 g CTAB) to 31 nm (0.2 g CTAB).

In Fig. 3a, the TEM studies of the hydrothermal sample without CTAB show that the product is made up of nanoparticles and nanowires. It indicates that the reaction is incomplete without CTAB surfactant. Indeed, the highly crystallized nanowires (rods) shown in the picture have been identified by selected

TABLE I
Effect of CTAB contents on the composition of LSMO nanoparticles.

Content of CTAB [g]	[CTAB]/[LSMO]	Composition [mole ratio]		
		La	Sr	Mn
0	0	0.16	0.83	0.92
0.05	0.21	0.40	0.6	0.95
0.10	0.41	0.36	0.63	0.95
0.20	0.82	0.30	0.70	1.01

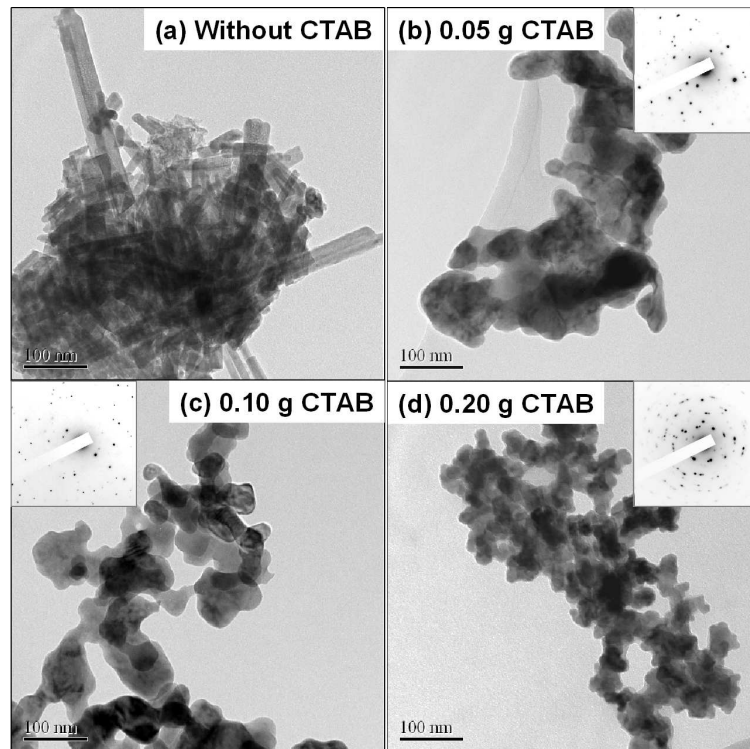


Fig. 3. The TEM photographs of LSMO powders obtained with (a) no CTAB, (b) 0.05 g CTAB, (c) 0.1 g CTAB and (d) 0.2 g CTAB. The inserted image is its electron diffraction.

area diffraction (SAD) and energy dispersive X-ray (EDX) to be $\text{La}(\text{OH})_3$. Figure 3b and c reveals the formation of LSMO particles. The particle size is relatively large and has a broad distribution. In Fig. 3d, small particles of narrow size distribution are obtained with 0.2 g CTAB treatment.

One important control parameter in the synthesis of mixed valence manganites with adjustable doping levels is the average oxidation state of the Mn ion [15]. The analysis of the LSMO powders by EDX shows the chemical composition. The data are listed in Table I. For powder treated with a higher CTAB content, where the La, Sr, and Mn composition was closer to the stoichiometric ratio with 0.2 g CTAB added in the hydrothermal process, $\text{La}_{0.3}\text{Sr}_{0.7}\text{MnO}_3$ nanoparticles were obtained. Evidently the usage of CTAB surfactant plays a very important role in controlling the chemistry of hydrothermal process.

It is recognized that the magnetization in the manganese perovskite phase is very sensitive to the stoichiometry, atomic defects, oxygen content, and the $\text{Mn}^{3+}/\text{Mn}^{4+}$ ratio [16]. In our case, all the samples with surfactant CTAB exhibited clear ferromagnetic switching characterization at room temperature (in

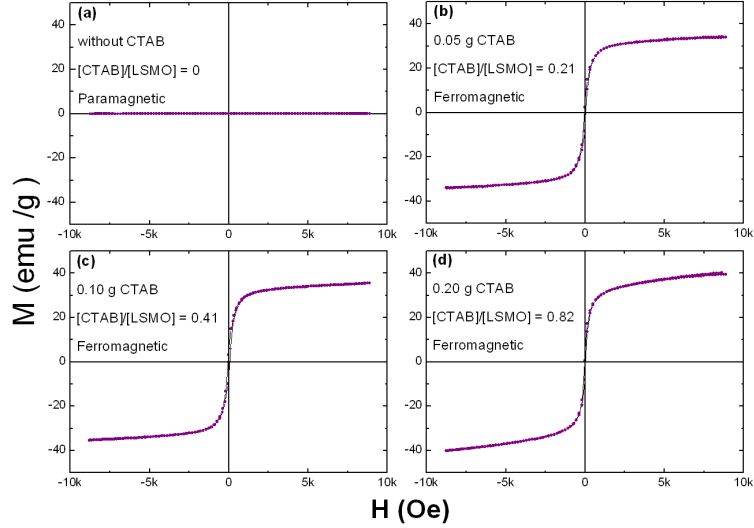


Fig. 4. The magnetization curve of LSMO powders obtained with (a) no CTAB, (b) 0.05 g CTAB, (c) 0.1 g CTAB and (d) 0.2 g CTAB.

TABLE II

Effect of CTAB contents on the magnetic properties of LSMO nanoparticles.

Content of CTAB [g]	[CTAB]/[LSMO]	Remanence magnetization [emu g ⁻¹]		Coercivity field [Oe]	
		MR ⁺	MR ⁻	H _C ⁺	H _C ⁻
0	0	-	-	-	-
0.05	0.21	4.46	-4.77	-56	49
0.10	0.41	5.18	-4.91	-66	54
0.20	0.82	3.03	-3.50	-30	30

Fig. 4b-d). Notably, in Fig. 4a, the LSMO without CTAB demonstrated diamagnetic properties although they are of good crystallinity. The coercivities of different samples are shown in Table II. As the content of CTAB in the hydrothermal process is increased, the coercivity decreased. It should also be noted that the exchange bias (H_C^+ and H_C^-) in the present system is symmetric about the zero field axis. It demonstrates that the $\text{La}_{0.3}\text{Sr}_{0.7}\text{MnO}_3$ nanoparticles are free of an antiferromagnetic layer.

4. Conclusions

In conclusion, we have successfully synthesized nanocrystalline $\text{La}_x\text{Sr}_{1-x}\text{MnO}_3$ by surfactant modified hydrothermal process. Powder XRD

patterns showed that the material is of a single phase perovskite structure when a proper amount of CTAB surfactant was used. A typical crystallite is in the range of several tens of nanometer. The as-prepared nano-sized LSMO particles are ferromagnetic and exhibit superparamagnetism at room temperature. Our results imply that the application of CTAB cationic surfactant has accelerated the solid state reaction, reducing the conventional formation temperature and reaction time.

Acknowledgments

This study was financed by the Hong Kong Research Grant Council and the Hong Kong Polytechnic University by its financial support (project codes: A-PE96, 5-ZH42 and RP97). The authors wish to thank Dr. K.H. Pang and Dr. X.H. Zhang and S.W. Cheung for their help in the experiment.

References

- [1] E. Dagotto, *Nanoscale Phase Separation and Colossal Magnetoresistance*, Springer, New York 2003, p. 1.
- [2] Y. Hou, J. Yu, S. Gao, *J. Mater. Chem.* **13**, 1983 (2003).
- [3] W.D. Yang, Y.H. Chang, S.H. Huang, *J. Eur. Ceram. Soc.* **25**, 3611 (2005).
- [4] G. Popov, S.V. Kalinin, R.A. Alvarez, M. Greenblatt, D.A. Bonnell, in: *Solid-State Chemistry of Inorganic Materials III*, Eds. M.J. Geselbracht, J.E. Greedan, D.C. Johnson, M.A. Subramanian, Vol. 658, MRS, Warrendale (PA) 2001, p. 39722.
- [5] A.P. Rao, D. Lavric, T.K. Nath, C.B. Eorn, L. Wu, F. Tsui, *Appl. Phys. Lett.* **73**, 3294 (1998).
- [6] A.M. Haghiri-Gosnet, J.P. Renard, *J. Phys. D, Appl. Phys.* **36**, 127 (2003).
- [7] M. Bowen, M. Bibes, A. Barthélémy, J.P. Contour, A. Anane, Y. Lemaitre, A. Fert, *Appl. Phys. Lett.* **82**, 233 (2003).
- [8] E.L. Nagaev, *Phys. Rep.* **346**, 387 (2001).
- [9] D. Grossin, J.G. Noudem, *Solid State Sci.* **6**, 939 (2004).
- [10] V. Uskoković, M. Drogenik, *Mater. Des.* **28**, 667 (2005).
- [11] A. Hassini, M. Gervais, S. Roger, P. Simon, J. Lecomte, N. Rainmboux, F. Gervais, *Solid State Sci.* **4**, 907 (2002).
- [12] J. Fang, J. Wang, S.C. Ng, C.H. Chew, L.M. Gan, *J. Mater. Sci.* **34**, 1943 (1999).
- [13] J. Spooren, R.J. Walton, F. Millange, *J. Mater. Chem.* **15**, 1542 (2005).
- [14] J. Goodwin, *Colloids and Interfaces with Surfactants and Polymer*, Wiley, Chichester 2004, p. 20.
- [15] J. J. Urban, L. Ouyang, M.H. Jo, D.S. Wang, H. Park, *Nano Lett.* **4**, 1547 (2004).
- [16] S. Roy, I. Dubenko, D. Ederh, N. Ali, *J. Appl. Phys.* **96**, 1202 (2004).